Appl. Math. Mech. -Engl. Ed., **41**(9), 1303–1320 (2020)

APPLIED MATHEMATICS AND MECHANICS (ENGLISH EDITION)

https://doi.org/10.1007/s10483-020-2662-6

Transverse shear and normal deformation effects on vibration behaviors of functionally graded micro-beams*

Zhu SU[1,†], Lifeng WANG[1], Kaipeng SUN[2], Jie SUN[2]

1. State Key Laboratory of Mechanics and Control of Mechanical Structures, Nanjing University of Aeronautics and Astronautics, Nanjing 210016, China;
2. Shanghai Institute of Satellite Engineering, Shanghai 201109, China

(Received May 17, 2020 / Revised Jul. 13, 2020)

Abstract A quasi-three dimensional model is proposed for the vibration analysis of functionally graded (FG) micro-beams with general boundary conditions based on the modified strain gradient theory. To consider the effects of transverse shear and normal deformations, a general displacement field is achieved by relaxing the assumption of the constant transverse displacement through the thickness. The conventional beam theories including the classical beam theory, the first-order beam theory, and the higher-order beam theory are regarded as the special cases of this model. The material properties changing gradually along the thickness direction are calculated by the Mori-Tanaka scheme. The energy-based formulation is derived by a variational method integrated with the penalty function method, where the Chebyshev orthogonal polynomials are used as the basis function of the displacement variables. The formulation is validated by some comparative examples, and then the parametric studies are conducted to investigate the effects of transverse shear and normal deformations on vibration behaviors.

Key words quasi-three dimensional theory, modified strain gradient theory, functionally graded (FG) micro-beam, size effect, vibration, general boundary condition

Chinese Library Classification O321, O327
2010 Mathematics Subject Classification 74H45, 70J10

1 Introduction

As advanced composite materials, functionally graded (FG) materials possess distinctive features of gradually spatial changes in the material properties, which enable FG materials to avoid the stress concentration of conventional laminated composite materials. Besides, FG materials can satisfy the multi-functional requirements by a wide selection of material constituents.

* Citation: SU, Z., WANG, L. F., SUN, K. P., and SUN, J. Transverse shear and normal deformation effects on vibration behaviors of functionally graded micro-beams. *Applied Mathematics and Mechanics* (*English Edition*), **41**(9), 1303–1320 (2020) https://doi.org/10.1007/s10483-020-2662-6

† Corresponding author, E-mail: suzhu@nuaa.edu.cn

Project supported by the National Natural Science Foundation of China (Nos. 51805250 and 11602145), the Natural Science Foundation of Jiangsu Province of China (No. BK20180429), the China Postdoctoral Science Foundation (No. 2019M660114), and the Jiangsu Planned Projects for Postdoctoral Research Funds of China (No. 2019K054)

Consequently, FG materials are suitable for many engineering fields and considerable attention has been paid to the mechanical behaviors of FG structures[1–3]. Recently, with the advancement in micro-electro-mechanical systems (MEMSs), FG materials have been utilized to build various micro-structures in order to achieve high performance, which encourage researchers to investigate and predict the mechanical behaviors of FG micro-structures. In most cases, micro-beams usually serve as the fundamental structures and the principal functional components in MEMSs[4–6]. As a consequence, it is of significance to provide insight into the dynamic behaviors of FG micro-beams before the design.

Since the size effect will arise and become a key factor affecting mechanical behaviors when the feature size of structures reduces to micron or even sub-micron levels[7–9], the size-dependent problems of micro-structures have been widely investigated by means of experiments, molecular dynamics simulations, and higher-order continuum theories[10–11]. However, owing to high modeling efficiency and low computational cost, higher-order continuum theories have extensive applications, in which the couple stress theory (CST) and the strain gradient theory (SGT) are notable. The CST is simple and convenient to involve the size effect only by introducing two material length scale parameters to consider the rotation gradient[12]. A modified couple stress theory (MCST) was presented in Ref. [13] via creating the symmetrical couple stress tensor which made the number of material length scale parameters reduce from two to one. The SGT originates from the work of Mindlin[14–15]. The essential idea is the addition of the first or higher order strain gradients to the constitutive equations. In Ref. [16], the first-order strain gradient was further decomposed into stretch and rotation gradients. From this point of view, the SGT can degenerate to the CST. On this basis, Lam et al.[17] developed a modified strain gradient theory (MSGT) via a similar procedure used in Ref. [13].

In recent years, by incorporating the CST/SGT into conventional beam theories, many micro-beam models have been established for FG micro-beams, e.g., MCST/MSGT-based Euler-Bernoulli beam models[18–19], MCST/SGT-based Timoshenko beam models[20–21], and MCST/MSGT-based higher-order beam models[22–24]. It is noted that most of the existing micro-beam models neglect the transverse normal deformation effect by assuming constant transverse displacement across the thickness direction, which was originally developed for those structures made of isotropic materials. However, due to the existence of the strong variation of material properties along the thickness, the above assumption appears quite inappropriate for FG structures[25]. In order to take the transverse normal deformation effect into consideration, some quasi-three dimensional (3D) theories have been developed for the mechanical analysis of FG structures, which possess high accuracy with low computational cost. Among the above models, the representative beam models are hierarchical beam models based on the Carrera unified formulation (CUF)[26–27] and the quasi-3D beam model developed from a refined shear deformation theory[28–29]. Up to now, some researchers have extended those quasi-3D theories into the mechanical analysis of FG micro-beams. Trinh et al.[30] analyzed the size-dependent static and dynamic behaviors of simply supported FG micro-beams by the MCST-based quasi-3D beam theory. Later, they further presented a quasi-3D vibration solution for two-directional FG micro-beams[31]. Yu et al.[32–33] studied the bending and vibration behaviors of one/two-dimensional FG micro-beams with the MCST-based quasi-3D theory combined with an isogometric analysis. Karamanli and Aydogdu[34] presented the size-dependent quasi-3D vibration analysis of two-dimensional rotating FG sandwich porous micro-beams by the finite element method (FEM). Obviously, the research efforts on the size-dependent quasi-3D analysis of FG micro-beams are limited. To the authors' best knowledge, almost all of these existing studies are limited to the MCST. As pointed out by Lei et al.[24], the MCST usually underestimates the size effect since it only considers the rotation gradient.

The aim of this paper is to develop an MSGT-based quasi-3D micro-beam model for vibration problems of FG micro-beams with general boundary conditions. The energy-based formulation is derived by a variational method integrated with the penalty function method. Based on the

model, the effects of the dimensionless material length scale parameter, the length-to-thickness ratio, the gradient index, and the boundary conditions on the vibration characteristics of FG micro-beams are studied. By comparing the results obtained from different micro-beam theories, the effects of transverse shear and normal deformations on the vibration behavior are further investigated.

2 Theoretical formulation

2.1 Model description

Figure 1 shows a typical two-phase FG micro-beam, in which the material properties vary continuously and smoothly along the z-direction. According to the Mori-Tanaka scheme, the effective material properties are given as follows[20–22,24]:

$$\frac{K_{\mathrm{ef}}-K_2}{K_1-K_2}=\frac{V_1}{1+(1-V_1)(K_1-K_2)/(K_2+4G_2/3)}, \tag{1}$$

$$\frac{G_{\mathrm{ef}}-G_2}{G_1-G_2}=\frac{V_1}{1+(1-V_1)(G_1-G_2)/(G_2+G_2(9K_2+8G_2)/(6(K_2+2G_2)))}, \tag{2}$$

where the bulk modulus and the shear modulus are denoted by K and G, respectively, and the subscripts 1 and 2 represent the two different constituents used in FG materials, respectively. The volume fraction V_1 is

$$V_1=\left(\frac{z}{h}+\frac{1}{2}\right)^p, \tag{3}$$

where p represents the gradient index governing the spatial variation of material properties. Then, one can obtain the effective Young's modulus E_{ef} and Poisson's ratio μ_{ef} as follows[20]:

$$E_{\mathrm{ef}}=\frac{9K_{\mathrm{ef}}G_{\mathrm{ef}}}{3K_{\mathrm{ef}}+G_{\mathrm{ef}}},\quad \mu_{\mathrm{ef}}=\frac{3K_{\mathrm{ef}}-2G_{\mathrm{ef}}}{6K_{\mathrm{ef}}+2G_{\mathrm{ef}}}. \tag{4}$$

The effective mass density can be defined as follows:

$$\rho_{\mathrm{ef}}=V_1(\rho_1-\rho_2)+\rho_2. \tag{5}$$

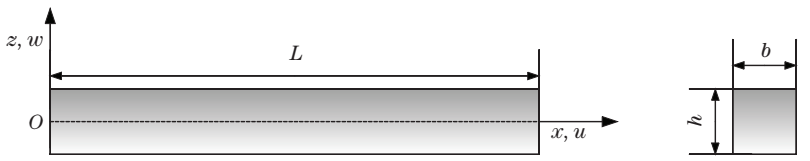

Fig. 1 Schematic diagram of an FG micro-beam

2.2 Kinematic and constitutive relations

A general displacement field, which can capture the transverse shear and normal deformation effects and has the capability of application to various beam theories, is defined as follows:

$$\begin{cases} u(x,z,t)=u_0(x,t)+f(z)\dfrac{\partial w_0}{\partial x}+g(z)u_1, \\ w=w_0+\phi(z)w_1, \end{cases} \tag{6}$$

where u_0 and w_0 denote the axial and transverse displacement components on the central line, respectively. u_1 is the rotation of the cross section with the shear effect, and w_1 is introduced to consider the transverse normal deformation effect. The shape functions $f(z)$, $g(z)$, and $\phi(z)$ govern the distributions of the strains and the stresses in the z-direction. By choosing appropriate shape functions, the displacement fields corresponding to various beam theories are easily obtained. For example, one can choose

$$f(z)=-z,\quad g(z)=0,\quad \phi(z)=0$$

for the classical beam theory (CBT);

$$f(z)=0,\quad g(z)=z,\quad \phi(z)=0$$

for the first-order beam theory (FBT); and

$$f(z)=-4z^3/(3h^2),\quad g(z)=z-4z^3/(3h^2),\quad \phi(z)=0$$

for Reddy's beam theory (RBT). In order to consider the transverse normal deformation effect, a quasi-3D beam theory is developed by choosing[28]

$$f(z)=-4z^3/(3h^2),\quad g(z)=z-4z^3/(3h^2),\quad \phi(z)=1-4z^2/h^2.$$

Using the above displacement field, non-zero linear strains can be obtained as follows:

$$\begin{cases}\epsilon_{11}=\dfrac{\partial u_0}{\partial x}+f\dfrac{\partial^2 w_0}{\partial x^2}+g\dfrac{\partial u_1}{\partial x},\quad \epsilon_{33}=\phi' w_1,\\ \epsilon_{13}=\epsilon_{31}=\dfrac{1}{2}\Big((f'+1)\dfrac{\partial w_0}{\partial x}+g'u_1+\phi\dfrac{\partial w_1}{\partial x}\Big),\end{cases}\tag{7}$$

in which the notation of prime is used to denote the derivative of shape functions.

In the MSGT, some additional higher-order deformation gradients, including the dilatation gradient tensor γ_i, the deviatoric stretch gradient tensor $\eta^{(1)}_{ijk}$, and the symmetric rotation gradient tensor χ^{s}_{ij}, are introduced to take the size effect into account, which are defined as follows[17]:

$$\gamma_i=\epsilon_{mm,i},\tag{8}$$

$$\begin{aligned}\eta^{(1)}_{ijk}=&\frac{1}{3}(\epsilon_{jk,i}+\epsilon_{ki,j}+\epsilon_{ij,k})-\frac{1}{15}\delta_{ij}(\epsilon_{mm,k}+2\epsilon_{mk,m})\\&-\frac{1}{15}\delta_{jk}(\epsilon_{mm,i}+2\epsilon_{mi,m})-\frac{1}{15}\delta_{ki}(\epsilon_{mm,j}+2\epsilon_{mj,m}),\end{aligned}\tag{9}$$

$$\chi^{\mathrm{s}}_{ij}=\frac{1}{2}(e_{ipq}\epsilon_{qj,p}+e_{jpq}\epsilon_{qi,p}),\tag{10}$$

in which a subscript preceded by a comma represents the differentiation with respect to the subscript. δ_{ij} and e_{ipq} denote the Kronecker delta and the permutation symbol, respectively. Then, substituting Eq. (7) into Eqs. (8)–(10) yields

$$\begin{cases}\gamma_1=\dfrac{\partial^2 u_0}{\partial x^2}+f\dfrac{\partial^3 w_0}{\partial x^3}+g\dfrac{\partial^2 u_1}{\partial x^2}+\phi'\dfrac{\partial w_1}{\partial x},\\ \gamma_3=f'\dfrac{\partial^2 w_0}{\partial x^2}+g'\dfrac{\partial u_1}{\partial x}+\phi'' w_1,\end{cases}\tag{11}$$

$$
\begin{cases}
\eta^{(1)}_{111} = \dfrac{2}{5}\Big(\dfrac{\partial^2 u_0}{\partial x^2} + f\dfrac{\partial^3 w_0}{\partial x^3} + g\dfrac{\partial^2 u_1}{\partial x^2}\Big) - \dfrac{1}{5}\Big(f''\dfrac{\partial w_0}{\partial x} + g'' u_1 + 2\phi'\dfrac{\partial w_1}{\partial x}\Big), \\
\eta^{(1)}_{333} = \dfrac{2}{5}\phi'' w_1 - \dfrac{1}{5}\Big((2f'+1)\dfrac{\partial^2 w_0}{\partial x^2} + 2g'\dfrac{\partial u_1}{\partial x} + \phi\dfrac{\partial^2 w_1}{\partial x^2}\Big), \\
\eta^{(1)}_{113} = \eta^{(1)}_{131} = \eta^{(1)}_{311} \\
\qquad = -\dfrac{1}{5}\phi'' w_1 + \dfrac{4}{15}\Big((2f'+1)\dfrac{\partial^2 w_0}{\partial x^2} + 2g'\dfrac{\partial u_1}{\partial x} + \phi\dfrac{\partial^2 w_1}{\partial x^2}\Big), \\
\eta^{(1)}_{223} = \eta^{(1)}_{232} = \eta^{(1)}_{322} \\
\qquad = -\dfrac{1}{5}\phi'' w_1 - \dfrac{1}{15}\Big((2f'+1)\dfrac{\partial^2 w_0}{\partial x^2} + 2g'\dfrac{\partial u_1}{\partial x} + \phi\dfrac{\partial^2 w_1}{\partial x^2}\Big), \\
\eta^{(1)}_{221} = \eta^{(1)}_{122} = \eta^{(1)}_{212} \\
\qquad = -\dfrac{1}{5}\Big(\dfrac{\partial^2 u_0}{\partial x^2} + f\dfrac{\partial^3 w_0}{\partial x^3} + g\dfrac{\partial^2 u_1}{\partial x^2}\Big) - \dfrac{1}{15}\Big(f''\dfrac{\partial w_0}{\partial x} + g'' u_1 + 2\phi'\dfrac{\partial w_1}{\partial x}\Big), \\
\eta^{(1)}_{331} = \eta^{(1)}_{133} = \eta^{(1)}_{313} \\
\qquad = -\dfrac{1}{5}\Big(\dfrac{\partial^2 u_0}{\partial x^2} + f\dfrac{\partial^3 w_0}{\partial x^3} + g\dfrac{\partial^2 u_1}{\partial x^2}\Big) + \dfrac{4}{15}\Big(f''\dfrac{\partial w_0}{\partial x} + g'' u_1 + 2\phi'\dfrac{\partial w_1}{\partial x}\Big),
\end{cases} \tag{12}
$$

$$
\begin{cases}
\chi^{\mathrm{s}}_{12} = \chi^{\mathrm{s}}_{21} = \dfrac{1}{4}\Big((f'-1)\dfrac{\partial^2 w_0}{\partial x^2} + g'\dfrac{\partial u_1}{\partial x} - \phi\dfrac{\partial^2 w_1}{\partial x^2}\Big), \\
\chi^{\mathrm{s}}_{23} = \chi^{\mathrm{s}}_{32} = \dfrac{1}{4}\Big(f''\dfrac{\partial w_0}{\partial x} + g'' u_1 - \phi'\dfrac{\partial w_1}{\partial x}\Big).
\end{cases} \tag{13}
$$

Although FG materials are globally heterogeneous, the locally effective properties at a given point can be assumed to be isotropic. Then, the classical and higher-order stresses are obtained by the following constitutive relations:

$$
\begin{cases}
\sigma_{ij} = \lambda_{\mathrm{ef}}\epsilon_{mm}\delta_{ij} + 2G_{\mathrm{ef}}\epsilon_{ij}, \quad p_i = 2G_{\mathrm{ef}} l_0^2 \gamma_i, \\
\tau^{(1)}_{ijk} = 2G_{\mathrm{ef}} l_1^2 \eta^{(1)}_{ijk}, \quad m^{\mathrm{s}}_{ij} = 2G_{\mathrm{ef}} l_2^2 \chi^{\mathrm{s}}_{ij},
\end{cases} \tag{14}
$$

where the Lamé parameter λ_{ef} is given by

$$
\lambda_{\mathrm{ef}} = E_{\mathrm{ef}}\mu_{\mathrm{ef}}/((1+\mu_{\mathrm{ef}})(1-2\mu_{\mathrm{ef}})).
$$

The symbols of l_0, l_1, and l_2 denote the material length scale parameters associated with those additional higher-order deformation gradients. When $l_0 = l_1 = 0\,\mu\mathrm{m}$, the MSGT can degenerate into the MCST.

2.3 Variational formulation

The energy functional for the FG micro-beam is defined as follows:

$$
\Pi = U + U_{\mathrm{bc}} - T, \tag{15}
$$

where the strain energy and the kinetic energy are represented by U and T, respectively. $U_{\rm bc}$ is the additional potential energy on the boundaries. The kinetic energy T is achieved by

$$\begin{aligned}T&=\frac{1}{2}\iiint_V\rho_{\rm ef}\Big(\Big(\frac{\partial u}{\partial t}\Big)^2+\Big(\frac{\partial w}{\partial t}\Big)^2\Big)\mathrm{d}V\\&=\frac{b}{2}\int_0^L I_1\Big(\Big(\frac{\partial u_0}{\partial t}\Big)^2+\Big(\frac{\partial w_0}{\partial t}\Big)^2\Big)+I_{ff}\Big(\frac{\partial^2 w_0}{\partial x\partial t}\Big)^2+I_{gg}\Big(\frac{\partial u_1}{\partial t}\Big)^2+I_{\phi\phi}\Big(\frac{\partial w_1}{\partial t}\Big)^2\\&\quad+2\Big(I_f\frac{\partial u_0}{\partial t}\frac{\partial^2 w_0}{\partial x\partial t}+I_g\frac{\partial u_0}{\partial t}\frac{\partial u_1}{\partial t}+I_{fg}\frac{\partial u_1}{\partial t}\frac{\partial^2 w_0}{\partial x\partial t}+I_\phi\frac{\partial w_0}{\partial t}\frac{\partial w_1}{\partial t}\Big)\mathrm{d}x,\end{aligned}\tag{16}$$

where

$$\begin{cases}I_1=\displaystyle\int_{-h/2}^{h/2}\rho_{\rm ef}\mathrm{d}z,\quad I_f=\int_{-h/2}^{h/2}\rho_{\rm ef}f\mathrm{d}z,\\[2ex]I_g=\displaystyle\int_{-h/2}^{h/2}\rho_{\rm ef}g\mathrm{d}z,\quad I_\phi=\int_{-h/2}^{h/2}\rho_{\rm ef}\phi\mathrm{d}z,\quad I_{fg}=\int_{-h/2}^{h/2}\rho_{\rm ef}fg\mathrm{d}z,\\[2ex]I_{ff}=\displaystyle\int_{-h/2}^{h/2}\rho_{\rm ef}ff\mathrm{d}z,\quad I_{gg}=\int_{-h/2}^{h/2}\rho_{\rm ef}gg\mathrm{d}z,\quad I_{\phi\phi}=\int_{-h/2}^{h/2}\rho_{\rm ef}\phi\phi\mathrm{d}z.\end{cases}$$

The strain energy U is calculated by the following integral equation[17]:

$$U=\frac{1}{2}\iiint_V(\sigma_{ij}\epsilon_{ij}+p_i\gamma_i+\tau_{ijk}^{(1)}\eta_{ijk}^{(1)}+m_{ij}\chi_{ij})\mathrm{d}V.\tag{17}$$

With the help of the force and moment resultants achieved by integrating the stresses in the z-direction (see Appendix A), the strain energy U is further written as follows:

$$\begin{aligned}U=&\frac{b}{2}\int_0^L\Big(N_{11}\frac{\partial u_0}{\partial x}+\Big(P_1+\frac{2}{5}T_{111}-\frac{3}{5}T_{221}-\frac{3}{5}T_{331}\Big)\frac{\partial^2 u_0}{\partial x^2}\\&-\Big(\frac{1}{5}T_{111}^{g''}+\frac{1}{5}T_{221}^{g''}-\frac{4}{5}T_{331}^{g''}-\frac{1}{2}Y_{23}^{g''}-N_{13}^{g'}\Big)u_1\\&+\Big(N_{11}^g+P_3^{g'}-\frac{2}{5}T_{333}^{g'}-\frac{2}{5}T_{223}^{g'}+\frac{8}{5}T_{113}^{g'}+\frac{1}{2}Y_{12}^{g'}\Big)\frac{\partial u_1}{\partial x}\\&+\Big(\frac{2}{5}T_{111}^g-\frac{3}{5}T_{221}^g-\frac{3}{5}T_{331}^g+P_1^g\Big)\frac{\partial^2 u_1}{\partial x^2}\\&+\Big(N_{13}^{f'+1}+\frac{1}{2}Y_{23}^{f''}-\frac{1}{5}T_{111}^{f''}-\frac{1}{5}T_{221}^{f''}+\frac{4}{5}T_{331}^{f''}\Big)\frac{\partial w_0}{\partial x}\\&+\Big(N_{11}^f+P_3^{f'}+\frac{1}{2}Y_{12}^{f'-1}-\frac{1}{5}T_{333}^{2f'+1}-\frac{1}{5}T_{223}^{2f'+1}+\frac{4}{5}T_{113}^{2f'+1}\Big)\frac{\partial^2 w_0}{\partial x^2}\\&+\Big(P_1^f+\frac{2}{5}T_{111}^f-\frac{3}{5}T_{221}^f-\frac{3}{5}T_{331}^f\Big)\frac{\partial^3 w_0}{\partial x^3}\\&+\Big(N_{33}^{\phi'}+P_3^{\phi''}+\frac{2}{5}T_{333}^{\phi''}-\frac{3}{5}T_{223}^{\phi''}-\frac{3}{5}T_{113}^{\phi''}\Big)w_1\\&+\Big(N_{13}^\phi+P_1^{\phi'}-\frac{2}{5}Y_{23}^{\phi'}-\frac{2}{5}T_{111}^{\phi'}-\frac{2}{5}T_{221}^{\phi'}+\frac{8}{5}T_{331}^{\phi'}\Big)\frac{\partial w_1}{\partial x}\\&+\Big(-\frac{1}{2}Y_{12}^\phi-\frac{1}{5}T_{333}^\phi-\frac{1}{5}T_{223}^\phi+\frac{4}{5}T_{113}^\phi\Big)\frac{\partial^2 w_1}{\partial x^2}\Big)\mathrm{d}x.\end{aligned}\tag{18}$$

The essential boundary conditions are enforced via the penalty function method. Introducing the penalty factors k yields the geometrical boundary conditions in the form of additional strain energy as follows[35–36]:

$$U_{\rm bc} = \frac{b}{2}\Big(k_1 u_0^2 + k_2 u_1^2 + k_3 w_0^2 + k_4 w_1^2 + k_5\Big(\frac{\partial u_0}{\partial x}\Big)^2 + k_6\Big(\frac{\partial u_1}{\partial x}\Big)^2 + k_7\Big(\frac{\partial w_0}{\partial x}\Big)^2 + k_8\Big(\frac{\partial w_1}{\partial x}\Big)^2 + k_9\Big(\frac{\partial^2 w_0}{\partial x^2}\Big)^2\Big). \tag{19}$$

It is noted that the penalty factors k_i (i = 1, 2, 3, 4, and 7) are associated with the classical boundary conditions obtained from the conventional continuum mechanics theory, and the other penalty factors are used to handle the higher-order boundary conditions resulting from the introduction of some additional higher-order deformation gradients and the corresponding high-order stress terms. The explicit relation between the penalty factors and the boundary conditions is achieved via the Hamilton principle as follows:

$$N_{11} - \frac{\partial P_1}{\partial x} - \frac{1}{5}\frac{\partial(2T_{111} - 3T_{221} - 3T_{331})}{\partial x} = k_1 u_0|_{x=0,L}, \tag{20}$$

$$N_{11}^g - \frac{\partial P_1^g}{\partial x} + P_3^{g'} + \frac{1}{5}\frac{\partial(2T_{111}^g - 3T_{221}^g - 3T_{331}^g)}{\partial x} - \frac{2}{5}(T_{333}^{g'} + T_{223}^{g'} - 4T_{113}^{g'}) + \frac{1}{2}Y_{12}^{g'} = k_2 u_1|_{x=0,L}, \tag{21}$$

$$N_{13}^{f'+1} - \frac{\partial N_1^f}{\partial x} - \frac{\partial P_3^{f'}}{\partial x} + \frac{\partial^2 P_1^f}{\partial x^2} + \frac{1}{5}(T_{111}^{f''} + T_{221}^{f''} - 4T_{331}^{f''}) + \frac{1}{2}Y_{23}^{f''} - \frac{1}{2}\frac{\partial Y_{12}^{f'-1}}{\partial x A} + \frac{1}{5}\frac{\partial(T_{333}^{2f'+1} + T_{223}^{2f'+1} - 4T_{113}^{2f'+1})}{\partial x} + \frac{1}{5}\frac{\partial^2(2T_{111}^f - 3T_{221}^f - 3T_{331}^f)}{\partial x^2} = k_3 w_0|_{x=0,L}, \tag{22}$$

$$N_{13}^{\phi} - \frac{2}{5}(T_{111}^{\phi'} + T_{221}^{\phi'} - 4T_{331}^{\phi'}) + \frac{1}{5}\frac{\partial(T_{333}^{\phi} + T_{223}^{\phi} - 4T_{113}^{\phi})}{\partial x} + P_1^{\phi'} + \frac{1}{2}\frac{\partial Y_{12}^{\phi}}{\partial x} - \frac{1}{2}Y_{23}^{\phi'} = k_4 w_1|_{x=0,L}, \tag{23}$$

$$P_1 + \frac{1}{5}(2T_{111} - 3T_{221} - 3T_{331}) = k_5\frac{\partial u_0}{\partial x}\Big|_{x=0,L}, \tag{24}$$

$$P_1^g + \frac{1}{5}(2T_{111}^g - 3T_{221}^g - 3T_{331}^g) = k_6\frac{\partial u_1}{\partial x}\Big|_{x=0,L}, \tag{25}$$

$$N_1^f + P_3^{f'} - \frac{\partial P_1^f}{\partial x} + \frac{1}{2}Y_{12}^{f'-1} - \frac{1}{5}(T_{333}^{2f'+1} + T_{223}^{2f'+1} - 4T_{113}^{2f'+1}) - \frac{1}{5}\frac{\partial(2T_{111}^f - 3T_{221}^f - 3T_{331}^f)}{\partial x} = k_7\frac{\partial w_0}{\partial x}\Big|_{x=0,L}, \tag{26}$$

$$\frac{1}{5}(T_{333}^{\phi} - T_{223}^{\phi} - 4T_{113}^{\phi}) + Y_{12}^{\phi} = k_8\frac{\partial w_1}{\partial x}\Big|_{x=0,L}, \tag{27}$$

$$P_1^f + \frac{1}{5}(2T_{111}^f - 3T_{221}^f - 3T_{331}^f) = k_9 \frac{\partial^2 w_0}{\partial x^2}\Big|_{x=0,L}. \tag{28}$$

It can be found that general boundary conditions are easily simulated by choosing appropriate values of penalty factors. In addition, the governing equations of motion are also achieved in this way, which are listed in Eqs. (A10)–(A13) of Appendix A.

2.4 Solution procedure

Using Chebyshev orthogonal polynomials as the basis function and implementing a linear coordinate transformation with $\xi = 2x/L - 1$, the displacement variables given in Eq. (6) are expressed as follows:

$$\begin{pmatrix} u_0(t,\xi) \\ u_1(t,\xi) \\ w_0(t,\xi) \\ w_1(t,\xi) \end{pmatrix} = \sum_{m=0}^{\infty} \begin{pmatrix} A_m(t) \\ B_m(t) \\ C_m(t) \\ D_m(t) \end{pmatrix} T_m(\xi) = \begin{pmatrix} \boldsymbol{A}^{\mathrm{T}}\boldsymbol{T} \\ \boldsymbol{B}^{\mathrm{T}}\boldsymbol{T} \\ \boldsymbol{C}^{\mathrm{T}}\boldsymbol{T} \\ \boldsymbol{D}^{\mathrm{T}}\boldsymbol{T} \end{pmatrix}, \tag{29}$$

where $\boldsymbol{A}$, $\boldsymbol{B}$, $\boldsymbol{C}$, and $\boldsymbol{D}$ denote the generalized coordinate variable vectors made up of A_m, B_m, C_m, and D_m, respectively. $T_m(\xi)$ is the one-dimensional mth-order Chebyshev orthogonal polynomial, which is achieved by

$$\begin{cases} T_0(\xi) = 1, \quad T_1(\xi) = \xi, \\ T_m(\xi) = 2\xi T_{m-1}(\xi) - T_{m-2}(\xi), \quad m \geqslant 2. \end{cases} \tag{30}$$

By inserting Eqs. (16)–(19) and (29) into Eq. (15) and applying the variational operation, one can obtain the following equation in the form of matrices:

$$\begin{pmatrix} \boldsymbol{M}_{u_0u_0} & \boldsymbol{M}_{u_0u_1} & \boldsymbol{M}_{u_0w_0} & \boldsymbol{0} \\ \boldsymbol{M}_{u_0u_1} & \boldsymbol{M}_{u_1u_1} & \boldsymbol{M}_{u_1w_0} & \boldsymbol{0} \\ \boldsymbol{M}_{u_0w_0} & \boldsymbol{M}_{u_1w_0} & \boldsymbol{M}_{w_0w_0} & \boldsymbol{M}_{w_0w_1} \\ \boldsymbol{0} & \boldsymbol{0} & \boldsymbol{M}_{w_0w_1} & \boldsymbol{M}_{w_1w_1} \end{pmatrix} \begin{pmatrix} \ddot{\boldsymbol{A}} \\ \ddot{\boldsymbol{B}} \\ \ddot{\boldsymbol{C}} \\ \ddot{\boldsymbol{D}} \end{pmatrix}$$

$$+ \begin{pmatrix} \boldsymbol{K}_{u_0u_0} & \boldsymbol{K}_{u_0u_1} & \boldsymbol{K}_{u_0w_0} & \boldsymbol{K}_{u_0w_1} \\ \boldsymbol{K}_{u_0u_1} & \boldsymbol{K}_{u_1u_1} & \boldsymbol{K}_{u_1w_0} & \boldsymbol{K}_{u_1w_1} \\ \boldsymbol{K}_{u_0w_0} & \boldsymbol{K}_{u_1w_0} & \boldsymbol{K}_{w_0w_0} & \boldsymbol{K}_{w_0w_1} \\ \boldsymbol{K}_{u_0w_1} & \boldsymbol{K}_{u_1w_1} & \boldsymbol{K}_{w_0w_1} & \boldsymbol{K}_{w_1w_1} \end{pmatrix} \begin{pmatrix} \boldsymbol{A} \\ \boldsymbol{B} \\ \boldsymbol{C} \\ \boldsymbol{D} \end{pmatrix} = \boldsymbol{0}. \tag{31}$$

The sub-matrices $\boldsymbol{M}_{u_0u_0}$ and $\boldsymbol{K}_{u_0u_0}$ are taken as examples to further clarify the calculation of the total mass and stiffness matrices. They are calculated by

$$\boldsymbol{M}_{u_0u_0} = \frac{LI_1}{2} \int_{-1}^{1} \boldsymbol{T}^{\mathrm{T}}\boldsymbol{T} \mathrm{d}(\xi), \tag{32}$$

$$\boldsymbol{K}_{u_0u_0} = \frac{2A_{11}}{L} \int_{-1}^{1} \frac{\mathrm{d}\boldsymbol{T}^{\mathrm{T}}}{\mathrm{d}\xi} \frac{\mathrm{d}\boldsymbol{T}}{\mathrm{d}\xi} \mathrm{d}\xi + \frac{16A_{66}}{L^3}\left(l_0^2 + \frac{2}{5}l_1^2\right) \int_{-1}^{1} \frac{\mathrm{d}^2\boldsymbol{T}^{\mathrm{T}}}{\mathrm{d}\xi^2} \frac{\mathrm{d}^2\boldsymbol{T}}{\mathrm{d}\xi^2} \mathrm{d}\xi, \tag{33}$$

where

$$A_{11} = \int_{-h/2}^{h/2} (\lambda_{\mathrm{ef}} + 2G_{\mathrm{ef}}) \mathrm{d}z, \quad A_{66} = \int_{-h/2}^{h/2} 2G_{\mathrm{ef}} \mathrm{d}z.$$

With the aid of assumption of a harmonic motion, one can obtain the standard characteristic equations from Eq. (31). It is noted that the characteristic equations corresponding to the CBT, the FBT, and the RBT can be achieved by moving the lines and columns of the total mass and stiffness matrices corresponding to the absent displacement variables.

3 Numerical examples

A wide range of numerical examples are given to verify the convergence, the accuracy, and the stability of this formulation. Unless otherwise specified, the FG materials are made of SiC with[32]

$$E_1 = 427\,\text{GPa}, \quad \mu_1 = 0.17, \quad \rho_1 = 3\,100\,\text{kg/m}^3$$

and Al with

$$E_2 = 70\,\text{GPa}, \quad \mu_2 = 0.3, \quad \rho_2 = 2\,702\,\text{kg/m}^3.$$

The material length scale parameters are taken as $l_0 = l_1 = l_2 = l = 15\,\mu\text{m}$ for the MSGT and $l_0 = l_1 = 0\,\mu\text{m}$, $l_2 = l = 15\,\mu\text{m}$ for the MCST. The boundary conditions, including the clamped, simply supported, and free boundary conditions and their arbitrary combinations, are considered[24,31].

The clamped boundary conditions are defined as follows:

$$\begin{cases} u_0 = 0, \quad u_1 = 0, \quad w_0 = 0, \quad w_1 = 0, \quad \dfrac{\partial u_0}{\partial x} = 0, \\ \dfrac{\partial u_1}{\partial x} = 0, \quad \dfrac{\partial w_0}{\partial x} = 0, \quad \dfrac{\partial w_1}{\partial x} = 0, \quad \dfrac{\partial^2 w_0}{\partial x^2} = 0. \end{cases}$$

The simply supported boundary conditions are defined as follows:

$$\begin{cases} w_0 = 0, \quad w_1 = 0, \\ \dfrac{\partial u_0}{\partial x} = 0, \quad \dfrac{\partial u_1}{\partial x} = 0, \quad \dfrac{\partial^2 w_0}{\partial x^2} = 0. \end{cases} \tag{34}$$

Note that the free boundary conditions represent no constraints at edges. For the sake of convenience, the dimensionless frequency parameter is defined as $\Omega = \omega L\sqrt{I_{10}/A_{110}}$, where A_{110} and I_{10} represent the values of A_{11} and I_1 of a homogeneous metal (Al) beam.

3.1 Convergence studies

The accuracy and efficiency of this formulation depend on both the numbers of terms of the Chebyshev orthogonal polynomials taken for the displacement variables and the values of the penalty factors for modeling the boundary conditions. Therefore, those two key parameters need to be studied before going into the analysis. In fact, the larger the number of the orthogonal polynomial terms used in Eq. (29), the more accurate the obtained results. However, for computational efficiency, the appropriate truncated number M needs to be determined to achieve the results with acceptable accuracy.

Table 1 presents the first eight dimensionless frequencies of completely free FG micro-beams having $h/l = 2, 8$, $L/h = 5$, and $p = 1$. An excellent convergence behavior can be found from those results. It can be seen that adopting $M = 12$ can obtain quite stable and acceptable results.

Theoretically, the penalty factors are taken as zero for free constraints whereas infinity for clamped constraints. However, the actual calculation cannot deal with infinite values and taking a very large value for the penalty factor may lead to round-off errors or ill-conditioning. Consequently, the determination of the penalty factors is further carried out. For the interest of convenience, the penalty factors are normalized by

$$\begin{cases} \Gamma_i = \lg \dfrac{k_i}{A_{110}}, \quad i = 1, 2, 3, 4, \\ \Gamma_i = \lg \dfrac{k_i}{A_{660}(l_0^2 + l_1^2)}, \quad i = 5, 6, 9, \\ \Gamma_i = \lg \dfrac{k_i}{A_{660}(l_1^2 + l_2^2)}, \quad i = 7, 8. \end{cases}$$

Table 1 Convergence of dimensionless frequencies of completely free FG micro-beams with different M, where $L/h = 5$, and $p = 1$

h/l	M	Ω_1	Ω_2	Ω_3	Ω_4	Ω_5	Ω_6	Ω_7	Ω_8
2	4	3.188 6	4.730 4	9.275 3	11.033	19.558	22.804	24.625	29.800
	6	3.157 9	4.697 7	7.801 8	10.233	14.184	17.387	23.792	26.578
	8	3.157 8	4.697 0	7.675 7	10.205	13.488	17.095	20.798	24.995
	10	3.157 7	4.697 0	7.674 5	10.204	13.471	17.084	20.040	24.850
	12	3.157 7	4.697 0	7.674 1	10.204	13.470	17.084	20.008	24.835
	14	3.157 7	4.697 0	7.674 0	10.204	13.470	17.084	20.00 6	24.834
8	4	1.676 1	4.523 4	4.869 7	9.162 0	9.793 8	14.183	16.273	18.391
	6	1.664 0	3.979 9	4.511 4	6.979 8	8.971 5	12.709	13.588	15.166
	8	1.664 0	3.931 6	4.510 4	6.685 3	8.871 5	10.154	12.981	13.562
	10	1.664 0	3.931 5	4.510 3	6.679 3	8.831 5	9.752 8	12.409	13.410
	12	1.663 9	3.931 4	4.510 3	6.678 8	8.829 8	9.736 2	12.359	13.400
	14	1.663 9	3.931 4	4.510 3	6.678 7	8.829 8	9.735 5	12.357	13.400

Figure 2 plots the effects of normalized penalty factors on dimensionless frequencies of FG micro-beams. It should be pointed out that appropriate values for the normalized penalty factors of Γ_i ($i = 1, 2, 3, 5, 6, 7$) are in accord with those in Ref. [35], where the MSGT-based FBT was used. For brevity, the corresponding figures related to the above penalty factors are

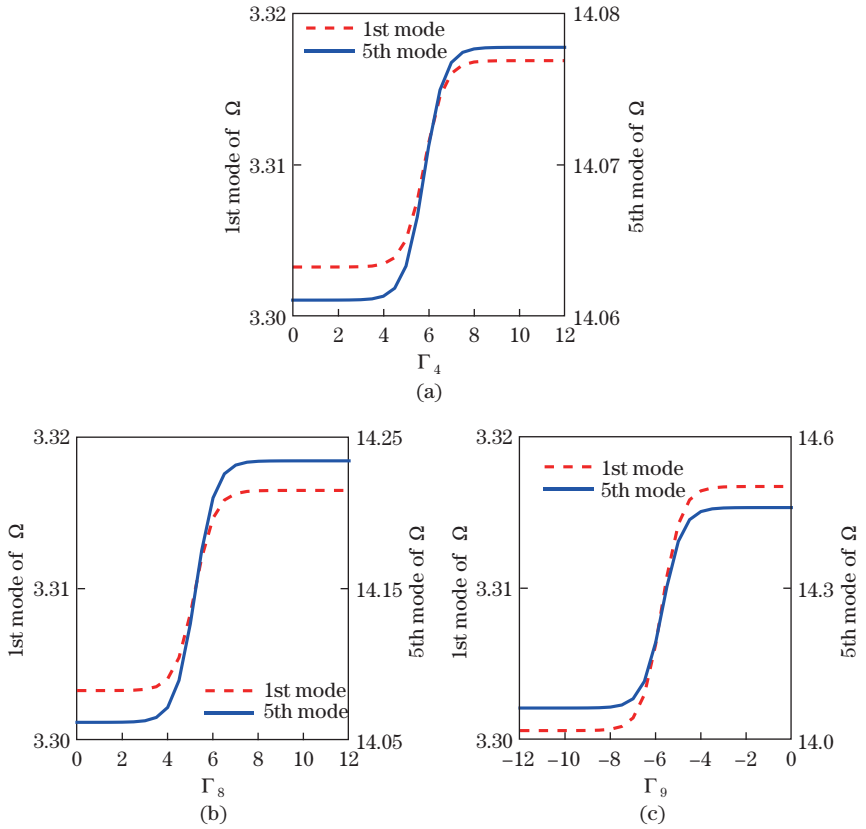

Fig. 2 Effects of the normalized penalty factors on the dimensionless frequencies of FG micro-beams, where $h/l = 2$, $L/h = 5$, and $p = 1$ (color online)

not shown in Fig. 2. In this analysis, the aforementioned six kinds of penalty factors are set to

$$\Gamma_1 = \Gamma_3 = \Gamma_5 = \Gamma_7 = 10, \quad \Gamma_2 = \Gamma_6 = 0$$

for clamped boundary conditions. For penalty factors of $\Gamma_i\,(i = 4, 8, 9)$, the 1st and 5th dimensionless frequencies are obtained by changing only one kind of penalty factors from small to large and assigning the others with zeros. It can be observed from Fig. 2 that, as the normalized penalty factor continually increases, all obtained results slightly increase, and finally keep a constant level. Accordingly, the appropriate values of the normalized penalty factors are defined as

$$\Gamma_4 = \Gamma_8 = 10, \quad \Gamma_9 = 0$$

for clamped boundary conditions.

3.2 Verification studies

To validate this formulation, some comparative examples are given. Due to lack of available quasi-3D results for FG micro-beams based on the MSGT, the numerical comparison for FG micro-beams within the frame of the MCST is firstly conducted. The dimensionless fundamental frequencies of simply supported FG micro-beams having $L/h = 10$ are listed in Table 2. This problem has been analyzed by Trinh et al.[30] via the Navier solution based on various beam theories including the CBT, the FBT, the RBT, and the quasi-3D method. Those calculated results have excellent consistency with the referred date, which not only verifies the accuracy of the present formulation, but also shows that it has the ability to accommodate various beam theories.

Table 2 Comparison of dimensionless fundamental frequencies of simply supported FG micro-beams, where $L/h = 10$

h/l	Theory	$p = 0.3$		$p = 1$		$p = 3$		$p = 10$	
		Ref. [30]	Present	Ref. [30]	Present	Ref. [30]	Present	Ref. [30]	Present
1	CBT	12.900 1	12.899 7	10.648 3	10.647 5	8.942 0	8.941 5	7.801 5	7.801 3
	FBT	12.605 5	12.605 5	10.398 3	10.398 3	8.711 1	8.711 1	7.584 0	7.584 0
	RBT	12.833 3	12.833 3	10.601 0	10.601 0	8.904 9	8.904 9	7.764 4	7.764 4
	Quasi-3D	12.742 2	12.742 2	10.509 3	10.509 3	8.793 6	8.793 6	7.623 6	7.623 6
2	CBT	7.930 3	7.930 1	6.616 0	6.615 5	5.736 2	5.735 9	5.123 4	5.123 3
	FBT	7.822 9	7.822 9	6.521 1	6.521 1	5.638 3	5.638 3	5.024 0	5.024 0
	RBT	7.871 8	7.871 8	6.567 1	6.567 1	5.687 7	5.687 7	5.073 4	5.073 4
	Quasi-3D	7.750 4	7.750 4	6.442 9	6.442 9	5.536 3	5.536 3	4.881 6	4.881 6
4	CBT	6.083 5	6.083 3	5.134 8	5.134 4	4.597 8	4.597 5	4.194 7	4.194 7
	FBT	6.011 0	6.011 0	5.069 2	5.069 2	4.525 7	4.525 7	4.118 6	4.118 6
	RBT	6.023 1	6.023 1	5.078 4	5.078 4	4.532 7	4.532 7	4.127 8	4.127 8
	Quasi-3D	5.872 6	5.872 6	4.926 2	4.926 2	4.353 3	4.353 3	3.902 9	3.902 9
8	CBT	5.526 2	5.526 0	4.692 0	4.691 7	4.266 0	4.265 7	3.928 4	3.928 3
	FBT	5.461 2	5.461 2	4.632 8	4.632 8	4.199 6	4.199 6	3.857 5	3.857 5
	RBT	5.464 0	5.464 0	4.631 4	4.631 4	4.192 2	4.192 2	3.853 1	3.853 1
	Quasi-3D	5.300 1	5.300 1	4.467 1	4.467 1	4.002 2	4.002 2	3.616 3	3.616 3

Table 3 presents the first ten dimensionless quasi-3D frequencies of simply supported FG micro-beams made of Al_2O_3 and Al. The used parameters in this analysis are

$$p = 1, \quad L/h = 10, \quad h/l = 1, 4, 20, 100.$$

Table 3 Comparison of first ten dimensionless quasi-3D frequencies of simply supported FG micro-beams (p=1, L/h=10)

Mode	$h/l=1$		$h/l=4$		$h/l=20$		$h/l=100$	
	Ref.[32]	Present	Ref.[32]	Present	Ref.[32]	Present	Ref.[32]	Present
1	10.627 8	10.627 8	4.846 2	4.846 2	4.213 7	4.213 7	4.186 5	4.186 5
2	26.230 4	26.230 7	18.568 1	18.568 1	16.115 0	16.115 0	16.008 6	16.008 6
3	41.326 1	41.326 1	26.223 2	26.223 2	26.038 3	26.037 5	26.026 8	26.026 0
4	78.595 2	78.596 0	39.999 8	39.999 8	34.617 9	34.617 8	34.387 0	34.386 9
5	88.945 5	88.945 4	66.437 5	66.437 8	57.027 2	57.027 4	56.615 0	56.615 2
6	131.057	131.058	78.739 9	78.740 3	77.908 6	77.906 9	77.802 8	77.801 2
7	149.550	149.551	97.670 3	97.678 3	83.599 6	83.605 6	83.048 5	83.054 2
8	183.405	183.406	129.142	129.394	110.653	111.113	109.743	110.186
9	219.865	219.882	133.485	134.001	130.513	130.593	130.415	130.511
10	235.827	235.832	168.146	170.928	140.540	142.681	139.350	141.440

The quasi-3D solutions provided by Yu et al.[32] by using the isogeometric analysis (IGA) are also listed in this table. Excellent agreement even for higher-order frequencies is observed from the results.

To further validate this formulation, Table 4 presents the dimensionless fundamental frequencies of FG micro-beams subjected to different boundary conditions based on the MSGT. The obtained results are compared with those given by Ansari et al.[21] by using the MSGT-based Timoshenko beam model and the generalized differential quadrature (GDQ) method. It is noted that in Ref. [21], the immovable simply supported boundary conditions were used. In order to better verify the present method, the same boundary conditions are considered. As expected, good agreement is found when adopting the same beam theory for all boundary conditions considered.

Table 4 Comparison of dimensionless fundamental frequencies of FG micro-beams with different boundary conditions, where $h/l=2$, $L/h=10$, S_1S_1 means immovable simply supported-immovable simply supported, CC means clamped-clamped, and CS_1 means clamped-immovable simply supported

Boundary condition		p						
		0.1	0.2	0.6	1.2	2	5	10
S_1S_1	Ref. [21]	0.956 0	0.893 2	0.768 3	0.686 7	0.631 9	0.553 5	0.513 1
	FBT	0.958 3	0.895 6	0.770 6	0.688 9	0.634 0	0.555 5	0.514 8
	Quasi-3D	0.884 9	0.826 6	0.712 6	0.638 4	0.588 4	0.514 8	0.474 8
CC	Ref. [21]	2.028 2	1.888 4	1.609 7	1.431 4	1.316 1	1.158 1	1.078 0
	FBT	2.034 5	1.895 2	1.615 5	1.435 8	1.319 7	1.161 2	1.080 9
	Quasi-3D	2.099 2	1.955 5	1.675 2	1.498 4	1.384 1	1.223 1	1.134 5
CS_1	Ref. [21]	1.449 6	1.350 7	1.153 6	1.027 1	0.944 9	0.831 5	0.773 7
	FBT	1.453 6	1.355 1	1.157 4	1.030 0	0.947 3	0.833 7	0.775 8
	Quasi-3D	1.417 1	1.320 6	1.131 5	1.011 3	0.93 29	0.822 2	0.762 1

3.3 Parametric studies

After the success of numerical comparison, the present formulation is used to study the effects of the key parameters on the vibration behaviors of FG micro-beams. In Figs. 3–5, SS presents simply supported-simply supported, CC presents clamped-clamped, CS presents clamped-simply supported, and CF presents clamped-free.

Figure 3 depicts the effects of the dimensionless material length scale parameter h/l on the vibration frequencies of FG micro-beams having $L/h = 10$ and $p = 1$. For all cases, the dimensionless frequency parameters of FG micro-beams decrease as h/l increases. This lies on the fact that the size effects become weak as h/l increases, leading to the reduction in the flexural rigidity. By comparing the frequencies obtained from the FBT and the RBT, it can be clearly seen that their differences are notable when h/l is small and are diminishing as h/l increases. It may be deduced that the strong size effects lead to failure of the FBT for moderately thick micro-beams with $L/h = 10$, particularly for clamped-clamped and clamped-simply supported boundary conditions. By making a comparison of the RBT and quasi-3D results, it also can be observed that the quasi-3D results are always smaller than the RBT ones. This is attributable to the normal deformation effect. Another interesting point is that there exists an intersection of two curve lines related to the FBT and quasi-3D results and the value of h/l corresponding to the intersection point is strongly affected by the boundary conditions.

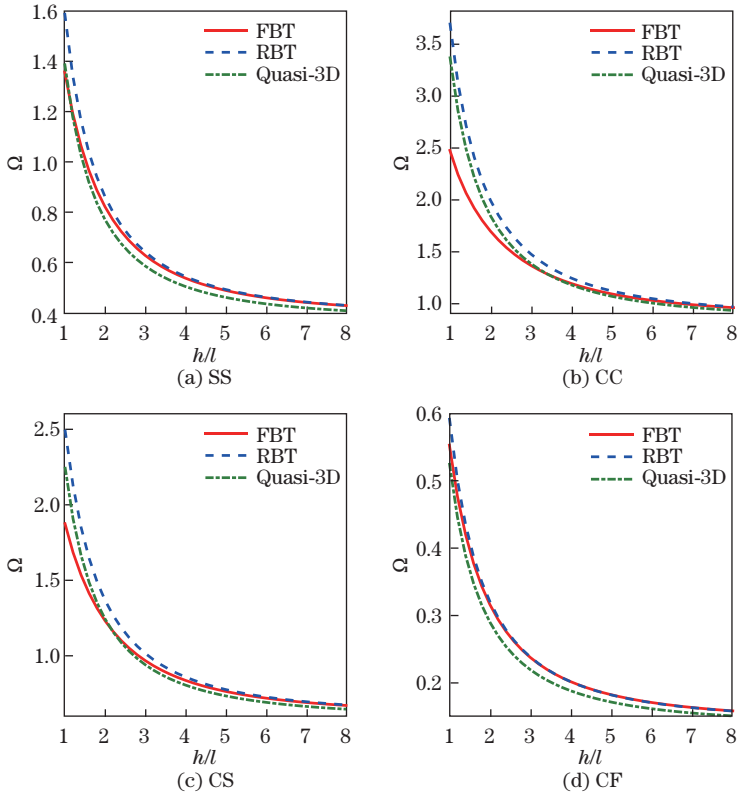

Fig. 3 Effects of the dimensionless material length scale parameter h/l on the dimensionless fundamental frequencies of FG micro-beams, where $L/h = 10$, and $p = 1$ (color online)

Figure 4 plots the effects of the gradient index p on the dimensionless fundamental frequency parameters for FG micro-beams having $h/l = 2$ and $L/h = 10$. As expected, the frequency parameters of FG micro-beams decrease for all cases as p increases. This reason is that the increase in the gradient index p results in the lessening of the volume fraction of SiC, leading to the reduction in the flexural rigidity. It also can be observed that the change of the gradient index p does not affect the order relation of the results from different beam theories when other parameters are fixed. The effects of the length-to-thickness ratio L/h on the vibration frequency parameters of FG micro-beams having $h/l = 2$ and $p = 1$ are shown in Fig. 5.

For all cases, the dimensionless frequency parameters of FG micro-beams decrease as the

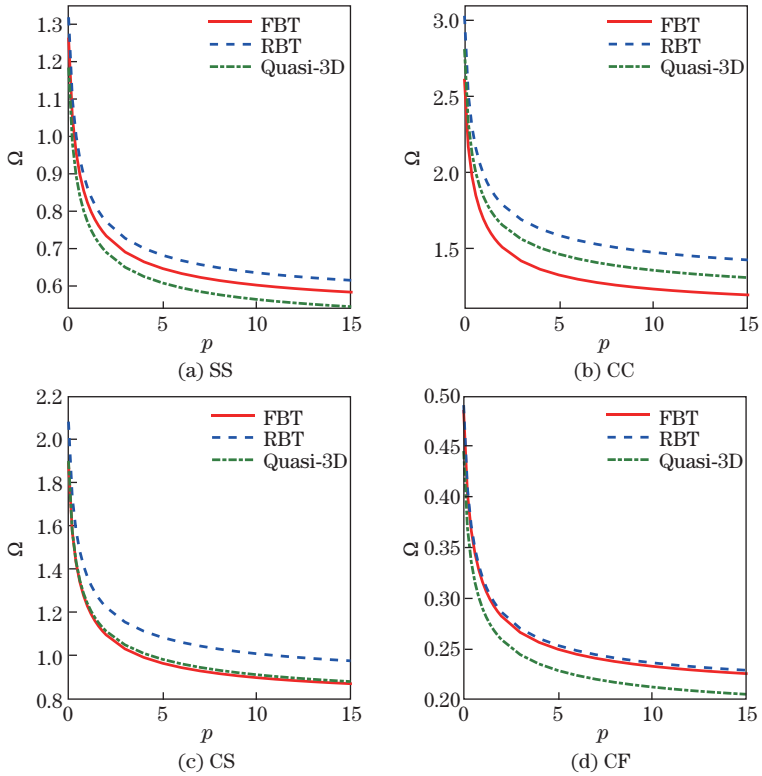

Fig. 4 Effects of the gradient index p on the dimensionless fundamental frequencies of FG micro-beams, where $L/h = 10$, and $h/l = 2$

length-to-thickness ratio increases. This is because the increase in L/h leads to the reduction in the flexural rigidity. The differences of the FBT and RBT results decrease as L/h increases, indicating that the FBT is not valid for slightly thick micro-beams, especially for clamped-clamped and clamped-simply supported boundary conditions.

4 Conclusions

This paper develops an MSGT-based quasi-3D micro-beam model for the vibration analysis of FG micro-beams. The effects of transverse shear and normal deformations are considered. The formulation is derived by a Chebyshev-based variational method combined with the penalty function method, in which the displacement field is given in a general form, which can be deduced to the CBT, the FBT, and the RBT. A wide range of examples on the vibration problems of FG micro-beams are presented. The results validate the present formulation. From parametric studies, it is observed that the dimensionless frequencies decrease with the increase in the dimensionless material length scale parameter h/l, the gradient index p, or the length-to-thickness ratio L/h, and the transverse shear effects play a significant role on vibration behaviors with lower values of h/l and L/h, particularly for clamped-clamped and clamped-simply supported boundary conditions. In addition, comparisons of the quasi-3D and RBT results indicate the transverse normal effects.

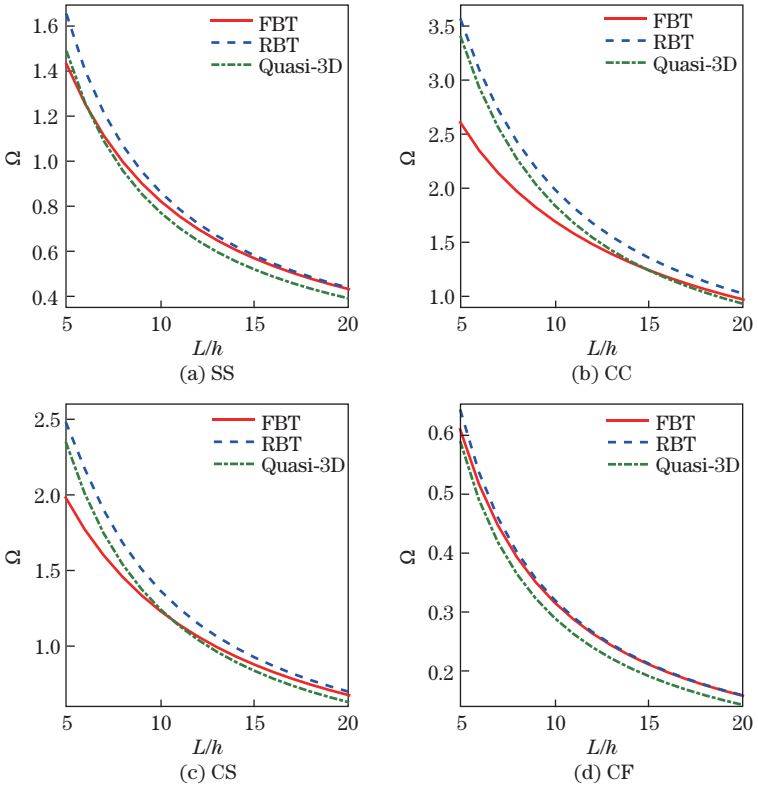

Fig. 5 Effects of the length-to-thickness ratio L/h on the dimensionless fundamental frequencies of FG micro-beams, where $h/l = 2$, and $p = 1$

References

[1] BIRMAN, V. and BYRD, L. W. Modeling and analysis of functionally graded materials and structures. *Applied Mechanics Reviews*, **60**, 195–216 (2007)

[2] ZHANG, N., KHAN, T., GUO, H. M., SHI, S. S., ZHONG, W., and ZHANG, W. W. Functionally graded materials: an overview of stability, buckling, and free vibration analysis. *Advances in Materials Science and Engineering*, **2019**, 1354150 (2019)

[3] GAYEN, D., TIWARI, R., and CHAKRABORTY, D. Static and dynamic analyses of cracked on functionally graded structural components: a review. *Composites Part B*: *Engineering*, **173**, 106982 (2019)

[4] SADEGHIAN, H., REZAZADEH, G., and OSTERBERG, P. M. Application of the generalized differential quadrature method to the study of pull-in phenomena of MEMS switches. *Journal of Microelectromechanical Systems*, **16**, 1334–1340 (2007)

[5] TAKAMATSU, H., FUKUNAGA, T., TANAKA, Y., KURATA, K., and TAKAHASHI, K. Micro-beam sensor for detection of thermal conductivity of gases and liquids. *Sensors and Actuators A*: *Physical*, **206**, 10–16 (2014)

[6] XIE, X., KONG, L., and WANG, Y. Coupled vibrations and frequency shift of compound system consisting of quartz crystal resonator in thickness-shear motions and micro-beam array immersed in liquid. *Applied Mathmatics and Mechanics* (*English Edition*), **36**(2), 225–232 (2015) https://doi.org/10.1007/s10483-015-1902-7

[7] FLECK, N. A., MULLER, G. M., ASHBY, M. F., and HUTCHINSON, J. W. Strain gradient plasticity: theory and experiment. *Acta Metallurgica et Materialia*, **42**, 475–487 (1994)

[8] MCFARLAND, A. W. and COLTON, J. S. Role of material microstructure in plate stiffness with relevance to microcantilever sensors. *Journal of Micromechanics and Microengineering*, **15**, 1060–1067 (2005)

[9] LEI, J., HE, Y. M., GUO, S., LI, Z. K., and LIU, D. B. Size-dependent vibration of nickel cantilever microbeams: experiment and gradient elasticity. *AIP Advances*, **6**, 105202 (2016)

[10] WANG, L. F. and HU, H. Y. Flexural wave propagation in single-walled carbon nanotubes. *Physical Review B*, **71**, 195412 (2005)

[11] THAI, H. T., VO, T. P., NGUYEN, T. K., and KIM, S. E. A review of continuum mechanics models for size-dependent analysis of beams and plates. *Composite Structures*, **177**, 196–219 (2017)

[12] MINDLIN, R. D. and TIERSTEN, H. F. Effects of couple-stresses in linear elasticity. *Archive for Rational Mechanics and Analysis*, **11**, 415–448 (1962)

[13] YANG, F., CHONG, A. C. M., LAM, D. C. C., and TONG, P. Couple stress based strain gradient theory for elasticity. *International Journal of Solids and Structures*, **39**, 2731–2743 (2002)

[14] MINDLIN, R. D. Second gradient of strain and surface-tension in linear elasticity. *International Journal of Solids and Structures*, **1**, 417–438 (1965)

[15] MINDLIN, R. D. and ESHEL, N. N. On first strain-gradient theories in linear elasticity. *International Journal of Solids and Structures*, **4**, 109–124 (1968)

[16] FLECK, N. A. and HUTCHINSON, J. W. A reformulation of strain gradient plasticity. *Journal of the Mechanics and Physics of Solids*, **49**, 2245–2271 (2001)

[17] LAM, D. C. C., YANG, F., CHONG, A. C. M., WANG, J., and TONG, P. Experiments and theory in strain gradient elasticity. *Journal of the Mechanics and Physics of Solids*, **51**, 1477–1508 (2003)

[18] ASGHARI, M., AHMADIAN, M. T., KAHROBAIYAN, M. H., and RAHAEIFARD, M. On the size-dependent behavior of functionally graded micro-beams. *Material and Design*, **31**, 2324–2329 (2010)

[19] AKGOZ, B. and CIVALEK, O. Buckling analysis of functionally graded microbeams based on the strain gradient theory. *Acta Mechanica*, **224**, 2185–2201 (2013)

[20] KE, L. L. and WANG, Y. S. Size effect on dynamic stability of functionally graded microbeams based on a modified couple stress theory. *Composite Structures*, **93**, 342–350 (2011)

[21] ANSARI, R., GHOLAMI, R., SHOJAEI, M. F., MOHAMMADI, V., and SAHMANI, S. Size-dependent bending, buckling and free vibration of functionally graded Timoshenko microbeams based on the most general strain gradient theory. *Composite Structures*, **100**, 385–397 (2013)

[22] SIMSEK, M. and REDDY, J. N. Bending and vibration of functionally graded microbeams using a new higher order beam theory and the modified couple stress theory. *International Journal of Engineering Science*, **64**, 37–53 (2013)

[23] LI, X. B., LI, L., and HU, Y. J. Instability of functionally graded micro-beams via micro-structure-dependent beam theory. *Applied Mathmatics and Mechanics* (*English Edition*), **39**(7), 923–952 (2018) https://doi.org/10.1007/s10483-018-2343-8

[24] LEI, J., HE, Y. M., ZHANG, B., GAN, Z. P., and ZENG, P. C. Bending and vibration of functionally graded sinusoidal microbeams based on the strain gradient elasticity theory. *International Journal of Engineering Science*, **72**, 36–52 (2013)

[25] CARRERA, E., BRISCHETTO, S., CINEFRA, M., and SOAVE, M. Effects of thickness stretching in functionally graded plates and shells. *Composites Part B*: *Engineering*, **42**, 123–133 (2011)

[26] GIUNTA, G., CRISAFULLI, D., BELOUETTAR, S., and CARRERA, E. Hierarchical theories for the free vibration analysis of functionally graded beams. *Composite Structures*, **94**, 68–74 (2011)

[27] MASHAT, D. S., CARRERA, E., ZENKOUR, A. M., AL KHATEEB, S. A., and FILIPPI, M. Free vibration of FGM layered beams by various theories and finite elements. *Composites Part B*: *Engineering*, **59**, 269–278 (2014)

[28] VO, T. P., THAI, H. T., NGUYEN, T. K., INAM, F., and LEE, J. A quasi-3D theory for vibration and buckling of functionally graded sandwich beams. *Composite Structures*, **119**, 1–12 (2015)

[29] VO, T. P., THAI, H. T., NGUYEN, T. K., INAM, F., and LEE, J. Static behaviour of functionally graded sandwich beams using a quasi-3D theory. *Composites Part B*: *Engineering*, **68**, 59–74 (2015)

[30] TRINH, L. C., NGUYEN, H. X., VO, T. P., and NGUYEN, T. K. Size-dependent behaviour of functionally graded microbeams using various shear deformation theories based on the modified couple stress theory. *Composite Structures*, **154**, 556–572 (2016)

[31] TRINH, L. C., VO, T. P., THAI, H. T., and NGUYEN, T. K. Size-dependent vibration of bi-directional functionally graded microbeams with arbitrary boundary conditions. *Composites Part B*: *Engineering*, **134**, 225–245 (2018)

[32] YU, T., HU, H. X., ZHANG, J., and BUI, T. Q. Isogeometric analysis of size-dependent effects for functionally graded microbeams by a non-classical quasi-3D theory. *Thin-Walled Structures*, **138**, 1–14 (2019)

[33] YU, T., ZHANG, J., HU, H., and BUI, T. Q. A novel size-dependent quasi-3D isogeometric beam model for two-directional FG microbeams analysis. *Composite Structures*, **211**, 76–88 (2019)

[34] KARAMANLI, A. and AYDOGDU, M. Size dependent flapwise vibration analysis of rotating two-directional functionally graded sandwich porous microbeams based on a transverse shear and normal deformation theory. *International Journal of Mechanical Sciences*, **159**, 165–181 (2019)

[35] SU, Z., JIN, G. Y., WANG, L. F., and WANG, D. Thermo-mechanical vibration analysis of size-dependent functionally graded micro-beams with general boundary conditions. *International Journal of Applied Mechanics*, **10**, 1850088 (2018)

[36] SU, Z., JIN, G. Y., and YE, T. G. Electro-mechanical vibration characteristics of functionally graded piezoelectric plates with general boundary conditions. *International Journal of Mechanical Sciences*, **138**, 42–53 (2018)

Appendix A

The force and moment resultants used are defined as follows:

$$(N_{11}, N_{11}^{f}, N_{11}^{g}) = \int_{-h/2}^{h/2} \sigma_{11}(1, f, g)\mathrm{d}z, \tag{A1}$$

$$N_{33}^{\phi'} = \int_{-h/2}^{h/2} \sigma_{33}\phi'\mathrm{d}z, \tag{A2}$$

$$(N_{13}^{f'+1}, N_{13}^{g'}, N_{13}^{\phi}) = \int_{-h/2}^{h/2} \sigma_{13}(f'+1, g', \phi)\mathrm{d}z, \tag{A3}$$

$$(P_1, P_1^{f}, P_1^{g}, P_1^{\phi'}) = \int_{-h/2}^{h/2} p_1(1, f, g, \phi')\mathrm{d}z, \tag{A4}$$

$$(P_3^{f'}, P_3^{g'}, P_3^{\phi''}) = \int_{-h/2}^{h/2} p_3(f', g', \phi'')\mathrm{d}z, \tag{A5}$$

$$\begin{aligned}&(T_{i1}, T_{i1}^{f}, T_{i1}^{g}, T_{i1}^{f''}, T_{i1}^{g''}, T_{i1}^{\phi'})\\ &= \int_{-h/2}^{h/2} \tau_i 1^{(1)}(1, f, g, f'', g'', \phi')\mathrm{d}z, \quad i = 11, 22, 33,\end{aligned} \tag{A6}$$

$$\begin{aligned}&(T_{i3}^{\phi}, T_{i3}^{2f'+1}, T_{i3}^{g'}, T_{i3}^{\phi''})\\ &= \int_{-h/2}^{h/2} \tau_i 3^{(1)}(\phi, 2f'+1, g', \phi'')\mathrm{d}z, \quad i = 11, 22, 33,\end{aligned} \tag{A7}$$

$$(Y_{12}^{\phi}, Y_{12}^{f'-1}, Y_{12}^{g'}) = \int_{-h/2}^{h/2} m_{12}^{\mathrm{s}}(\phi, f'-1, g')\mathrm{d}z, \tag{A8}$$

$$(Y_{23}^{\phi'}, Y_{23}^{f''}, Y_{23}^{g''}) = \int_{-h/2}^{h/2} m_{23}^{\mathrm{s}}(\phi', f'', g'')\mathrm{d}z. \tag{A9}$$

The governing equations of the FG micro-beam are obtained via the Hamilton principle as follows:

$$\begin{aligned}
&\frac{\partial N_{11}}{\partial x} - \frac{\partial^2 P_1}{\partial x^2} - \frac{1}{5}\frac{\partial^2 (2T_{111} - 3T_{221} - 3T_{331})}{\partial x^2} \\
&= I\frac{\partial^2 u_0}{\partial t^2} + I_g \frac{\partial^2 u_1}{\partial t^2} + I_f \frac{\partial^3 w_0}{\partial t^2 \partial x},
\end{aligned} \tag{A10}$$

$$\begin{aligned}
&\frac{\partial N_{11}^g}{\partial x} - N_{13}^{g'} - \frac{\partial^2 P_1^g}{\partial x^2} + \frac{\partial P_3^{g'}}{\partial x} - \frac{1}{5}\frac{\partial^2 (2T_{111}^g - 3T_{221}^g - 3T_{331}^g)}{\partial x^2} + \frac{1}{5}(T_{111}^{g'} + T_{221}^{g'} - 4T_{331}^{g'}) \\
&+ \frac{1}{2}\frac{\partial Y_{12}^{g'}}{\partial x} - \frac{1}{2}Y_{23}^{g'} - \frac{2}{5}\frac{\partial (T_{333}^{g'} + T_{223}^{g'} - 4T_{113}^{g'})}{\partial x} \\
&= I_g \frac{\partial^2 u_0}{\partial t^2} + I_{gg}\frac{\partial^2 u_1}{\partial t^2} + I_{fg}\frac{\partial^3 w_0}{\partial t^2 \partial x},
\end{aligned} \tag{A11}$$

$$\begin{aligned}
&\frac{\partial N_{13}^{f'+1}}{\partial x} - \frac{\partial^2 N_{11}^f}{\partial x^2} - \frac{\partial^2 P_3^{f'}}{\partial x^2} + \frac{\partial^3 P_1^f}{\partial x^3} - \frac{1}{5}\frac{\partial (T_{111}^{f''} + T_{221}^{f''} - 4T_{331}^{f''})}{\partial x} \\
&+ \frac{1}{5}\frac{\partial^2 (T_{333}^{2f'+1} + T_{223}^{2f'+1} - 4T_{113}^{2f'+1})}{\partial x^2} + \frac{1}{5}\frac{\partial^3 (T_{111}^f - 3T_{221}^f - 3T_{331}^f)}{\partial x^3} \\
&+ \frac{1}{2}\frac{\partial Y_{23}^{f''}}{\partial x} - \frac{1}{2}\frac{\partial^2 Y_{12}^{f'-1}}{\partial x^2} \\
&= I\frac{\partial^2 w_0}{\partial t^2} + I_\phi \frac{\partial^2 w_1}{\partial t^2} - I_f \frac{\partial^3 u_0}{\partial t^2 \partial x} - I_{fg}\frac{\partial^3 u_1}{\partial t^2 \partial x} - I_{ff}\frac{\partial^4 w_0}{\partial t^2 \partial x^2},
\end{aligned} \tag{A12}$$

$$\begin{aligned}
&\frac{\partial N_{13}^{\phi}}{\partial x} - N_{33}^{\phi'} - \frac{2}{5}\frac{\partial (T_{111}^{\phi'} + T_{221}^{\phi'} - 4T_{331}^{\phi'})}{\partial x} - \frac{1}{5}(T_{333}^{\phi''} + T_{223}^{\phi''} - 4T_{113}^{\phi''}) \\
&+ \frac{1}{5}\frac{\partial^2 (T_{333}^{\phi} + T_{223}^{\phi} - 4T_{113}^{\phi})}{\partial x^2} + \frac{\partial P_1^{\phi'}}{\partial x} - P_3^{\phi''} + \frac{1}{2}\frac{\partial Y_{12}^{\phi}}{\partial x^2} - \frac{\partial Y_{23}^{\phi}}{\partial x} \\
&= T_{\phi\phi}\frac{\partial^2 w_1}{\partial t^2} + I_\phi \frac{\partial^2 w_0}{\partial t^2}.
\end{aligned} \tag{A13}$$